RESPONSE OF SUPERHEATED EMULSION DETECTORS TO LOW ENERGY ALPHA IRRADIATION

T. Morlat[a], A.C. Fernandes[a], M. Felizardo[a], A. Kling[a], T. A. Girard[a,b], J.G. Marques[a], F.P. Carvalho[a] and C. Cruz[c]

[a] C^2TN, Centro de Ciências e Tecnologias Nucleares, Instituto Superior Técnico, Universidade de Lisboa, E.N. 10, 2695-066 Bobadela LRS,Portugal

[b] Departamento de Fisica, Universidade de Lisboa, 1749-016 Lisboa, Portugal

[c] Instituto de Plasmas e Fusão Nuclear, Instituto Superior Técnico, Universidade de Lisboa, E.N. 10, 2695-066 Bobadela LRS,Portugal

Abstract

Superheated Emulsion Detectors (SED) are traditionally employed in the detection of neutrons. In this work the focus is on the detection of alpha particles for an eventual alpha spectrometer using C_2ClF_5 as the target liquid. The alpha-droplet interaction is examined via computational studies, and a geometric model developed to describe the anticipated detector response. Experiments with alpha-emitting uranium- and samarium-doped SEDs at temperatures of 5-12 ºC confirm that the event rate is related to the size of the droplets, and are in model agreement for temperatures below 8ºC; above this temperature, the acoustic sensitivity is reduced by signal attenuation as a result of the increasing bubble population, for which the addition of an attenuation coefficient restores the agreement with experiment. The results suggest a SED-based alpha spectrometer.

1. INTRODUCTION

A SED consists of a distribution of micrometric, superheated liquid droplets in a gel-like medium. SEDs have been used to detect and study neutron the response of a variety of liquids [1-9] which arises via the constituent ion recoils from elastic neutron scattering. In this paper, we investigate their response to low energy alpha particles (α) of energy 2.25 – 4.72 MeV during temperature ramping**,** with a focus on the potential measurement of α-emissivity from ultralow activity integrated circuits for soft error qualification arising from naturally-occuring radioactivity in the materials.

The response of SEDs to α irradiations has been previously studied in Refs. [6-10], mostly however using either a uranium composite (U_3O_8) or ^{241}Am distributed in the gel matrix; the response to ^{226}Ra at various temperatures was examined in Ref. [9], and use of an external source was reported [11] using small CCl_2F_2 droplet sizes (3±1μm). The response of superheated C_4F_{10} emulsions to α has been studied

[12] by simulation using the GEANT3.21 toolkit, with the α contamination present either in the gel or both gel and active liquid.

This study focused on the SED response to the α-emitting elements uranium and samarium, with dominant energies E_α of 4.722 and 4.774 MeV for ^{234}U, 4.151 and 4.198 MeV for ^{238}U and 2.248 MeV for ^{147}Sm [13] using devices containing small diameter C_2ClF_5 droplets. The uranium mimics the natural radioactivity component of materials, with the samarium providing lower energy α .The contribution from α-decays of other natural isotopes can be neglected due to low natural abundance (^{235}U) or significantly longer half-lives (^{148}Sm, ^{149}Sm). The theoretical basis for the study is described in Sec. 2, which includes a model developed to describe the α–droplet interaction. The SED fabrication and set up are described in Sec. 3. The measurement results are discussed in Sec. 4 in terms of the model, and its modification for the attenuation of the acoustic signal. Conclusions are drawn in Sec. 5, to include the development of a possible α spectrometer.

2. THEORETICAL CONSIDERATIONS

The general physics of SED operation is based on the "thermal spike" model of Seitz [14]. Each superheated liquid droplet can undergo a phase transition to the vapor phase when a particle fulfills two nucleation conditions: its energy deposition is higher than the thermodynamic critical energy of the superheated liquid,

$$E \geq E_c = 4\pi R_c^2 (\sigma - T\frac{\partial\sigma}{\partial T}) + \frac{4\pi}{3} R_c^3 \rho_v h_v - \frac{4\pi}{3} R_c^3 \Delta p \quad , \qquad (1)$$

and the deposition must occur within a critical track length,

$$dE/dx \geq E_c/L_c \quad , \qquad (2)$$

where T is the SED operating temperature, σ is the surface tension of the bubble, ρ_v is the vapor density, $h_v(T) = h_l - h_v$ is the heat of vaporization, and $R_c = 2\sigma(T)/\Delta p$ where $\Delta p = p_v - p_l$ isthe difference pressure between the vapor p_v and liquid p_l. The E_c/L_c is the critical linear energy transfer (LET_c), required for bubble nucleation, with $L_c = \Lambda R_c$ the effective ionic energy deposition length, and Λ a liquid-dependent parameter : Λ(T,P) [14,8,9].

Fulfilment of these two conditions results in the explosive phase transition of the droplet, which is accompanied by a sound wave that is recorded by a microphone, and a visible bubble of ~ 1 mm diameter.

2.1 Bragg Curves

Although an α is itself a "recoiling" ^{4}He ion, the larger kinetic energy of α decay produces a significantly different track-averaged Bragg curve compared to an ion recoil produced in a scattering event [13]. The intersection between LET_C and the Bragg curve, which yields the minimum depth penetration ($p_<$) required for a nucleation, can be determined for uranium and samariumusing TRIM 2008 [15] for C_2ClF_5 at each temperature, and $\Lambda(T) = 4.3(\rho_l/\rho_v)^{1/3}$ where ρ_l is the liquid density. As indicated by the Bragg curve of Fig. 1, α's originating on a droplet surface would generally achieve $LET > LET_c$ in C_2ClF_5 over distances of several tens of μm in the liquid, following several tens of μm penetrations with $LET < LET_c$. Droplets with diameters $\leq p_<$ cannot contribute since the α traverses the droplet without achieving LET_c; droplets with diameters beyond $p_>$ will also contribute despite that the LET is again $< LET_c$ since the bubble nucleation has already been triggered.

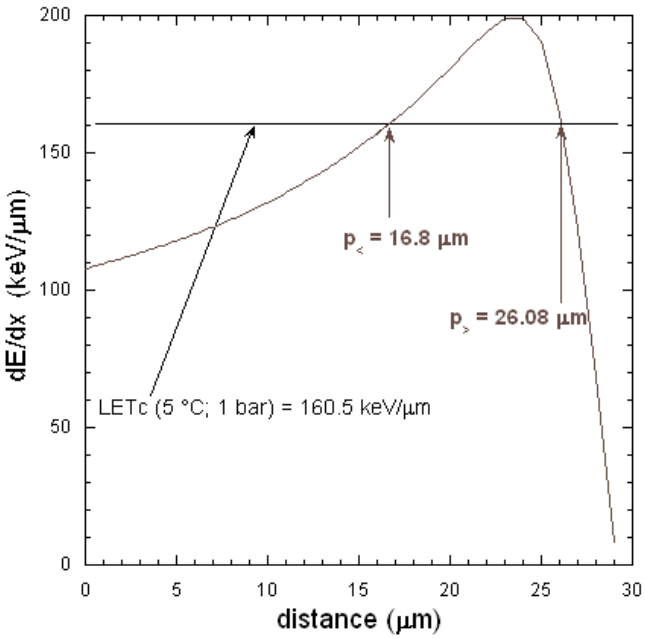

Fig. 1: SRIM-computed Bragg curve in C_2ClF_5 for an α of 4.198 MeV at 5 °C and ambient pressure. The intersection between the LET_c (160.5 keV/μm) and the curve gives $p_<$ (16.8 μm) and $p_>$ (26.1 μm).

In the case of the α-emitter doping, the U_3O_8 and Sm_2O_3 both have an electrochemical affinity for both C_2ClF_5 [16-18]. In consequence, they should migrate towards the droplet surfaces to preferentially populate the droplet surfaces; at the least, larger droplets should have a larger number of α-emitters, hence higher decay probability. The ions have moreover an affinity for the hydrophobic surface of the droplets, hence do not penetrate and in fact stabilize the emulsion by acting as a surfactant [10].

The dependence of $p_<$ on the liquid temperature, for the most intense E_α emitted by the uranium and samarium solutions, is shown in Figs. 2. From Fig. 2(a), for a fixed droplet size, the ^{234}U α emitters should begin triggering the droplets at ~ 2 °C higher temperature than the ^{238}U α emitters, which would

provide an increase in the event rate with temperature ramping. From Fig. 2(b), the ^{147}Sm α should be able to trigger droplets of diameters > 1.5 µm, and a flat response in the counting rate while ramping the temperature from 5-12 °C at ambient pressure could be expected. The case of uranium is more complicated: four α-energies are involved. If we choose as an example a 10 µm-diameter droplet, from 5-7 °C a "low increase" response could be expected; above 8 °C, the event rate should then increase due to the participation of the ^{234}U α.

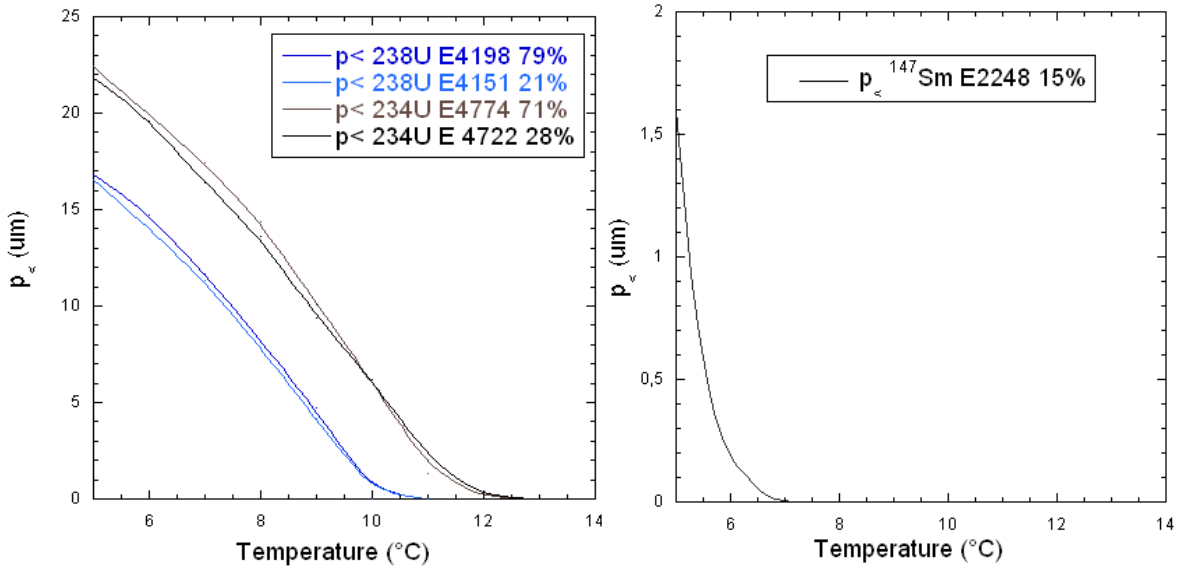

(a) (b)

Fig. 2: (a) Minimum penetration depth in C_2ClF_5 required for bubble nucleation by surface-generated (a) uranium and (b) samarium decay α's as a function of operating temperature. The ^{234}U α emitters begin their contribution at 2°C higher temperature than the ^{238}U α emitters for the same droplet size.

2.2 Model

In the case of surface emission, a model inspired by Ref. [8] and derived from the Bragg curves of the emitted α's in the $C_2ClF_5$is shown schematically in Fig. 3: its basis is the geometric intersection of two spheres with centers separated by a distance R, one of radius $p_<$ and the second with droplet radius R.

From Fig. 3, $\cos(\alpha) = \frac{p_<}{2R}$: since $\theta_< + \beta = \pi$ and $\beta = \pi - 2\alpha$; $\cos(\theta_<) = 2\left(\frac{p_<}{2R}\right)^2 - 1$. Integrating $\theta \in [0;\theta_<]$ gives an overvalue of the "nucleation volume " (hatched in red in Fig. 3), requiring subtraction of the volume $\frac{1}{3}\pi h^2(3p_< - h)$, with $h = p_<(1 - \frac{p_<}{2R})$.

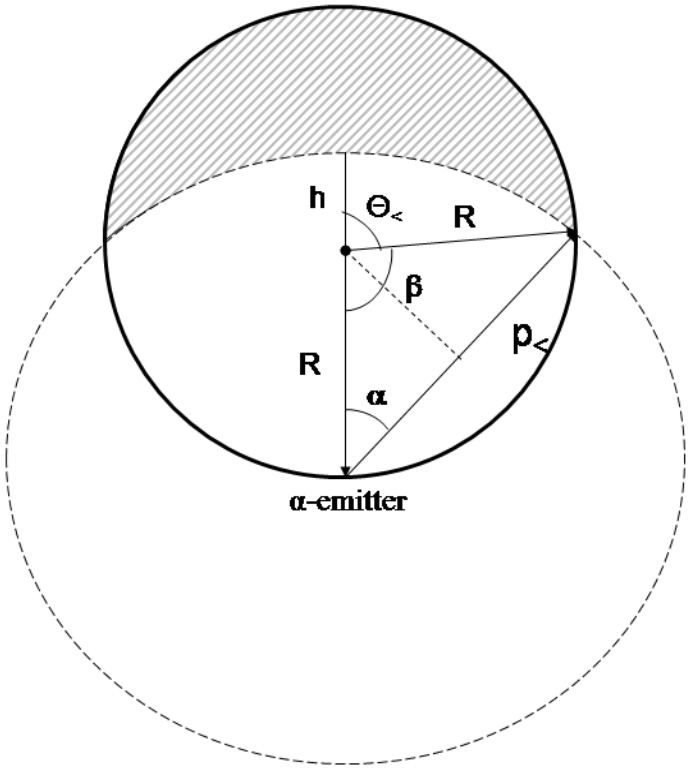

Fig. 3: schematic view of the minimum penetration depth in relation to the droplet, showing that alpha events may be triggered well inside the liquid (shaded), especially at increasing energies.

A bubble nucleation efficiency can be written as the ratio of the hatched volume (including the subtraction of cap volume) and the droplet volume:

$$\varepsilon_{nuc}(p_< : R) = \frac{\frac{2\pi R^3}{3}\int_0^{\theta_<} \sin\vartheta d\vartheta}{\frac{4\pi}{3}R^3} - \frac{\frac{\pi}{3}p_<^3(1-\frac{p_<}{2R})^2(2+\frac{p_<}{2R})}{\frac{4\pi}{3}R^3}$$

$$= 1 - \left(\frac{\mathrm{p}_<}{2\mathrm{R}}\right)^2 - 2(\frac{\mathrm{p}_<}{2\mathrm{R}})^3(1-\frac{\mathrm{p}_<}{2\mathrm{R}})^2(2+\frac{\mathrm{p}_<}{2\mathrm{R}}) \quad , \qquad (3)$$

When the nucleation efficiency is convolved with the droplet size distribution, represented by a Gaussian (<R> = 5.5 μm and σ = 5 μm), an overall efficiency curve is obtained. In the case of Fig. 4 for an α from ^{238}U, the curve shows that only the largest droplets undergo nucleations at ≥ 5 °C.

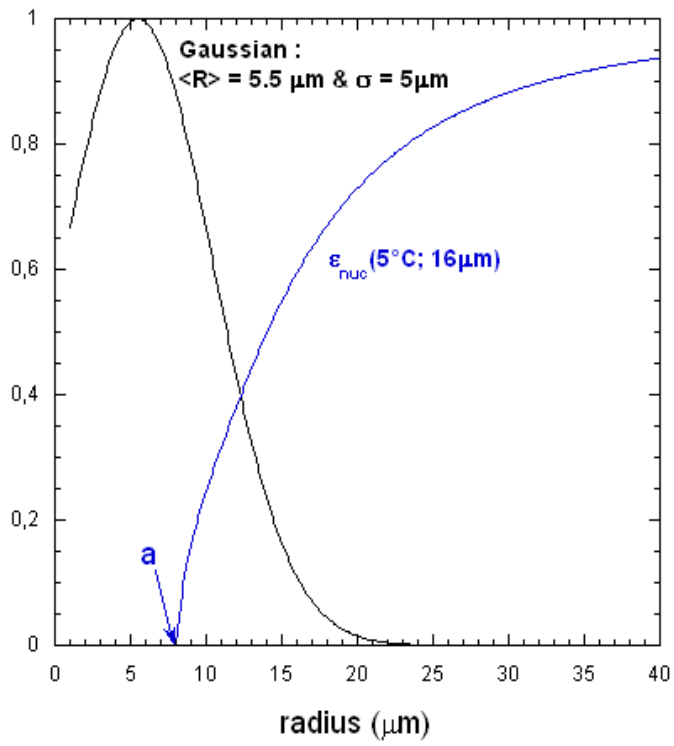

Fig. 4 : Nucleation efficiency of a SED at 5 °C ($p_< = 16\,\mu m$) for 4.198 MeV α's (^{238}U) in the example droplet distribution.

The SED counting rate at each temperature (corresponding to a specific value of $p_<$) is given by:

$$\tau_\alpha(p_< \leftrightarrow T) = \frac{1}{2} A_0 \sum_{k_a} f_{k_a} \varepsilon(p_<) F(p_<) \quad , \qquad (4)$$

where the prefactor assumes that all uranium decay occurs at the droplet surface [9], A_0 is the activity injected and f_{ka} is the number of alphas per unit activity inside the SED, ε is the average nucleation efficiency (calculated for each temperature ↔ $p_<$ and involved droplet sizes):

$$\varepsilon(p_<) = \frac{\int_a^\infty \varepsilon_{nuc}(p_<; R)\left(e^{-\frac{(R-<R>)^2}{2\sigma^2}}\right) dR}{\int_0^\infty e^{-\frac{(R-<R>)^2}{2\sigma^2}} dR} \quad , \qquad (5)$$

F is a "number of droplets" efficiency, or the number of droplets that were involved in nucleation at each temperature; it corresponds to the area beneath the droplet distribution when bubble nucleation begins:

$$F(p_<) = \frac{\int_a^\infty e^{-\frac{(R-<R>)^2}{2\sigma^2}} dR}{\int_0^\infty e^{-\frac{(R-<R>)^2}{2\sigma^2}} dR} \quad . \qquad (6)$$

3. EXPERIMENTAL VERIFICATIONS

3.1 Fabrication Protocol

The SEDs were scaled-down 150 mL versions of the standard SIMPLE SED, prepared following standard protocols [4] using 3-5 g of C_2ClF_5.

The detector gel was prepared by mixing 4.9 g gelatin + 19.5 g of bi-distilled water (bdw), and melting at 60 °C for 20 min; separately, 10 g of PolyVinylPyrrolidone (PVP) + 24.9 g of bdw were combined and also melted at 60 °C for 20 min. The gelatin and PVP solutions were then blended for 20 min at 60 °C, and 50.8 g of the concentrated gel added to 185.5 g of glycerin in a 150 ml bottle and heated at 80 °C for 1h30 with slow agitation. The hot gel was outgassed by vacuum dessication followed by bubble aspiration. This is a necessary step to remove all air trapped during the fabrication process: measurements showed that without outgassing, the response was flat as seen in Fig 5.

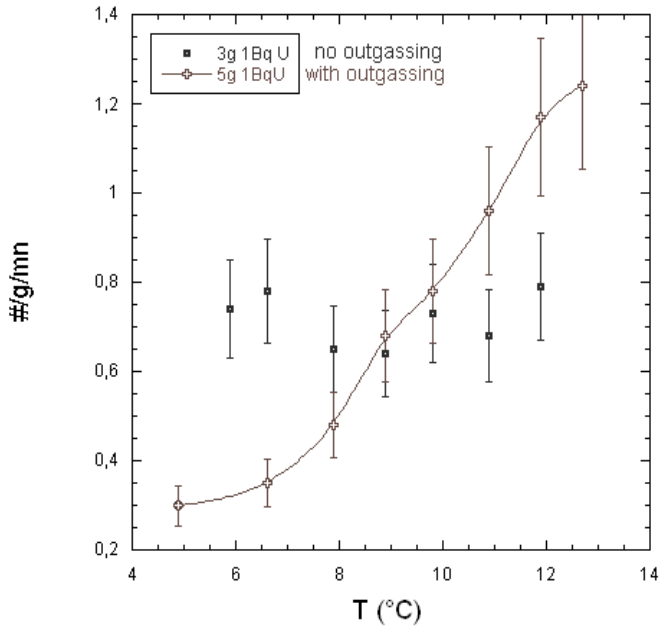

Fig. 5: counting rate of two SEDs doped with 1Bq U: black - SED without outgassing (3 g; 1 Bq; 0.7 evt/g/min); brown - SED with outgassing (the fit is to guide the eye).

A quantity of radioactive liquid source was then injected into the hot gel at 44 °C and agitated quickly before being placed inside the hyperbaric chamber at 20 bar for 4 h, with a stirring at 300 rpm to fractionate the liquid. The heater was then stopped for 1 h and the agitation slowed to 50 rpm. An hour later, the emulsions were cooled by cold water circulation at 5 °C for 12 hours, the pressure then slowly released and the SEDs extracted for use.

For the uranium solution (Uranium Standard solution in HNO_3 2-5% U =1.000 g/l ICP), the quantity was 300 µl (3.7 Bq); for the samarium (Sm_2O_3 in 5% HNO_3; Sm=10^4 µg/ml), 600 µl (0.37 Bq). To verify the actual α emission spectra from uranium and verify activities, the source α spectrum was measured with an α-spectrometer (OCtetePlus, ORTEC-EG&G with 450 mm^2 surface barrier detectors); the measured concentration agreed with the nominal value within ± 4%. Two radioisotopes were identified, ^{234}U and ^{238}U, with the same activity, indicating that the two isotopes were in equilibrium and yielding the emission of four α's (^{234}U: {4.77 MeV at 71%; 4.72 MeV at 28%} and ^{238}U: {4.20 MeV at 79%; 4.15 MeV at 21%}); the emission from ^{235}U was negligible. In the case of samarium, only one α (^{147}Sm {2.25 MeV at 100%}) was present.

Two additional SEDs were made (3.6 g, 3 Bq U and 3.0 g, 0.3 Bq U) with the same emulsion fabrication protocol, except that the gel temperature was increased to 52 °C with the intent of decreasing the droplet sizes.

3.2 Droplet Size Distribution

The DSDs were measured in randomly-selected slices of the gel matrices, taken from randomly-selected sites in the SED volumes, with an optical microscope (Olympus Bx 60M) as seen in Fig. 6. The results in each slice were similar, with the predominant radii ~ 5 µm for the 3.0g, 3 Bq U device, and predominant radii ~ 3.5 µm for the 3.6 g, 3 Bq U and 3.0 g, 0.3 Bq U.

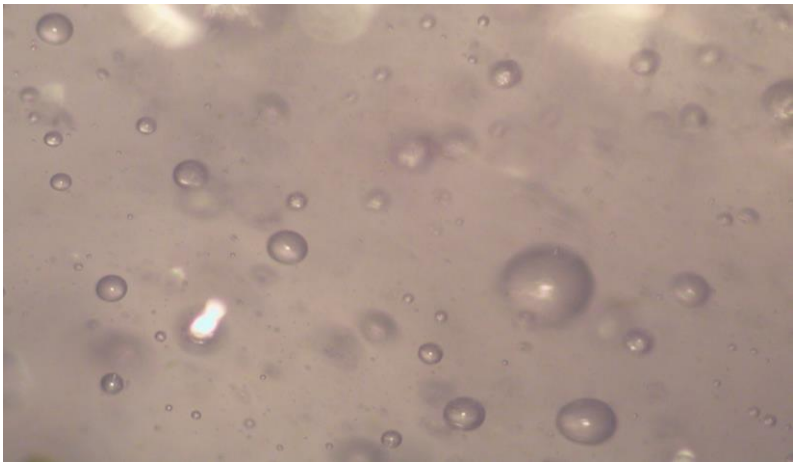

Fig. 6: a typical gel measurement slice from the 3.0 g, 3 Bq U SED. The droplet sizes are

non-uniform and present a distribution with a predominant radius of 5 µm.

The resulting DSDs were fit both with a Gaussian (mean value = 5 µm, σ = 5 µm) and a Lorentzian (mean value = 5 µm, width Γ = 6.92 µm). As seen in Fig. 7(a) for the 3.0 g, 3 Bq U device, the Gaussian does not include the droplets above 20 µm, which are included in the tail of the Lorentzian: the Lorentzian distribution is used hereafter. Similarly, the 3.6 g, 3 Bq U and 3.0 g, 0.3 Bq U devices yielded Lorentzians of mean value = 3.7 µm, Γ = 4.5 µm.

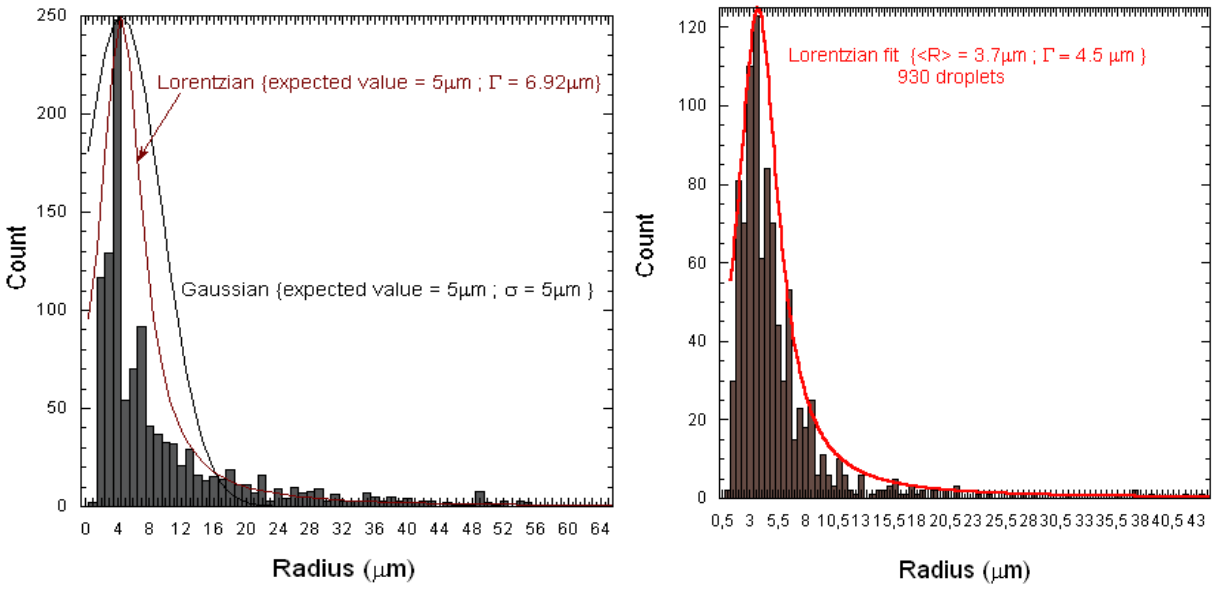

(a) (b)

Fig. 7: (a) experimental DSD (1162 droplets) of the 3.0 g, 3 Bq U SED together with its Gaussian (black) and Lorentzian (red) fits; (b) experimental DSD (930 droplets) DSDs for the 3.6 g, 3 Bq U and 3.0 g, 0.3 Bq U devices with Lorentzian fit.

3.3 Measurements

Each SED was placed inside a temperature-controlled, circulating water bath, surrounded by a radiation shielding (1 m x 0.8 m x 0.75 cm) made of concrete blocks (20 cm thick, 40 cm height) topped by paraffin (30 cm height) and polyethylene (1 m x 0.8 m x 0.05 m). Inside the shielding a 5 cm acoustic foam padding was installed to reduce the ambient noise (without this, only events with amplitudes higher than 2 mV were detected; with, events with amplitudes of 0.4 mV could be detected). The bath temperature was monitored with an undoped SED containing a temperature probe (IKA-Werke, PT 100), which also provided background measurements.

The SED responses were measured in atmospheric pressure at temperatures in steps of ~ 1 ºC between 5 – 12 °C (4.9 °C; 5.9 °C; 6.6 °C; 7.9 °C; 8.9 °C; 9.8 °C; 10.9 °C; 11.9 °C; above 13 °C, γ-ray nucleation sensitivity begins) for two activities of uranium and for 0.3 Bq of samarium. The time required for thermalization (uncertainty of ± 0.1 °C) between adjacent steps was of order 1-2 h. Signal acquisition began after thermalization, lasting from 20 min up to 1 h depending on the event rate. The acoustic instrumentation employed was the same as in the SIMPLE experiment [6]: acoustic signals were recorded by a top-mounted MCE-200 Panasonic microphone with a 0.020–16 kHz (3dB) range, with the data records screened with a MatLab digital band-pass filter for frequencies of 450-750 Hz [19] and amplitudes above the 0.2 mV noise level.

4. RESULTS & MODEL COMPARISONS

The response results in the case of the samarium doping are shown in Fig. 8, in events per unit time and liquid mass. As predicted by Fig. 2(b), only droplets with radius > 0.75 μm would contribute to "α nucleation" at 5 °C; above this temperature, any samarium α triggers any droplet, and there should be no increase in the counting rate because only one α is involved. The theoretical expression is in good agreement with the experimental result, giving a rate of 1.35 evt/g/min against the measured 1.28 ± 0.20 evt/g/min at 5 °C.

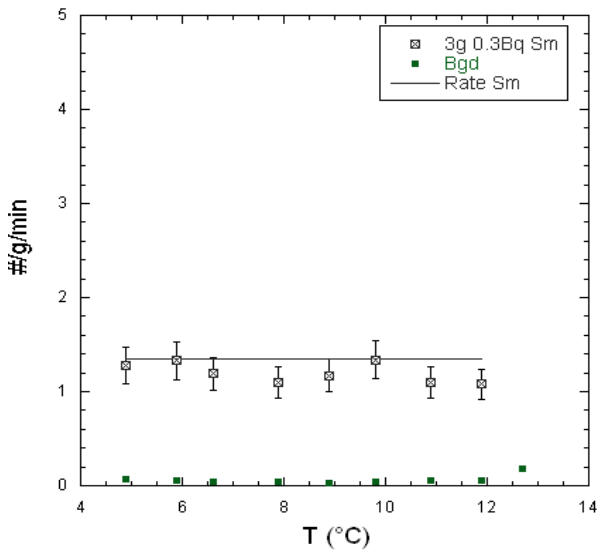

Fig. 8: Measured and calculated responses of a Sm-doped SED (3 g) as a function of temperature.

The results for the U-doped SEDs are shown in Fig. 9. In both cases, an event rate increase with temperature is observed, consistent with the reduction in nucleation threshold with increasing superheat. The event rates increase with the dopant activity, demonstrating that adding 10x more activity yields an event rate 10x higher (at 5 °C: 0.11± 0.03 evt/g/min for 0.3 Bq U vs. 1.02 ± 0.1 evt/g/min for 3 Bq U

(3.0 g)). Different event rates are however measured for the same nominal activity of different emitters (Fig. 9(a)).

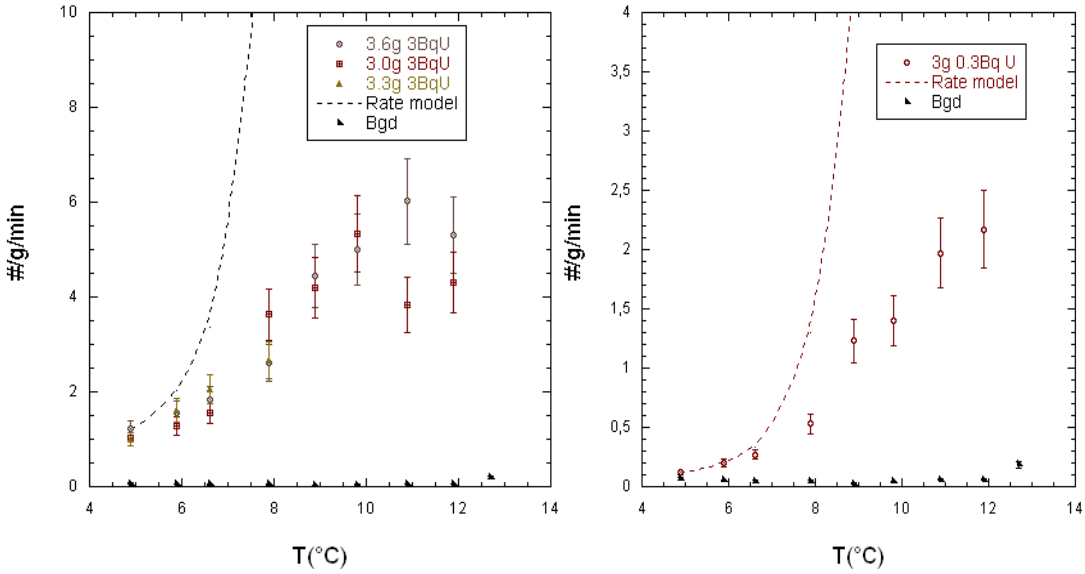

(a) (b)

Fig. 9: Measured and calculated responses of a U-doped SED as a function of temperature: (a) 3 Bq, the fit was done for a DSD centered at 3.7 µm in radius; (b) 0.3 Bq (3 g).

In the case of uranium, the event rate starts to increase rapidly above 7 ºC. The calculated response (dotted line) in Fig. 9 indicates that the contribution of ^{234}U begins above this temperature if a Lorentzian DSD centred at 3.7 µm diameter is assumed. The measured event rate increased by a factor of two (SED {3.0 g; 3 Bq U}: 1.57 ± 0.17 evt/g/min at 6.6 °C and 3.63 ± 0.50 evt/g/min at 7.9 °C), demonstrating that twice the number of α's is detected as expected due to the equilibrium of ^{234}U and ^{238}U activities.

4.1 Signal Filtering

The model and experimental rate results appear in good agreement for temperatures lower than 8 °C; above this temperature, the model predicts a higher event rate than observed.

A review of the experiments noted that visual inspections, before and after each run, observed more bubbles than recorded by the microphone. The main frequency of the acoustic signal was also seen to vary with temperature and accumulated SED exposure. The majority of the observed bubbles were of small diameter, which would yield correspondingly small signal amplitudes [8]. Re-tuning the band-pass filter frequency to 100-300 Hz reduced the noise level to about 0.2 mV, revealing a larger number of events hidden in the noise as seen in Fig. 10(b). This new acceptance window was found to contain the majority of event signals. It is lower than the previous window utilized (450-750 Hz), due to the

decrease of the droplet size distribution, but maintains the signal decay time constants of the event signals (5-40 ms) [19].

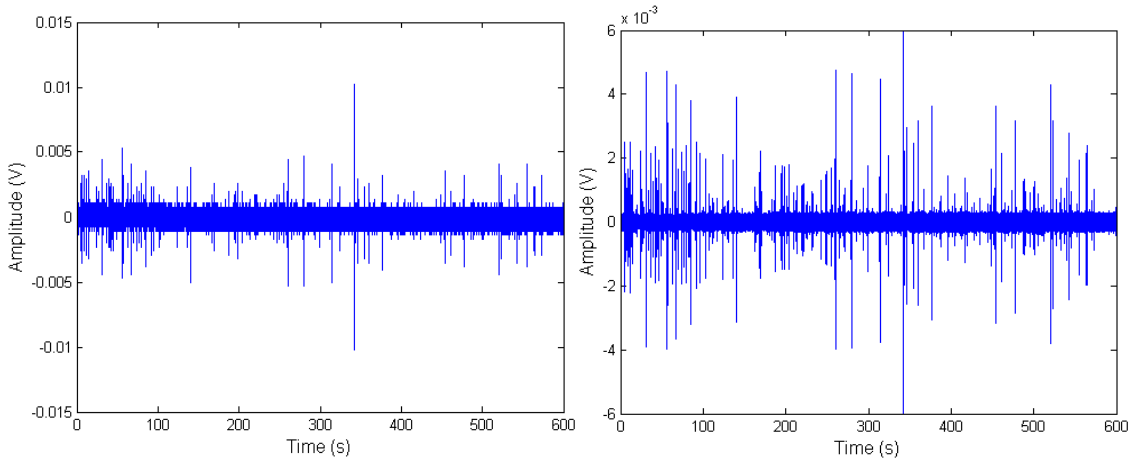

(a) (b)

Fig. 10: Acoustic signal with standard (a) and optimized (b) filtering routines of a U-doped SDD at 9 °C (3 g active mass). Each spike represents an event; (b) corresponds to 160 events for a 10 min file.

4.2 Signal Attenuation

Although the re-tuned frequency filtering provided some improvement, it continued to provide lower event rates above 8 °C than predicted by the model.

Previous studies [20-23] have suggested an acoustic signal attenuation caused by the increasing bubble population. The presence of bubbles with a volume fraction of 0.4% in a SED has a substantial effect on its acoustic properties [20], and reduces the velocity of sound at low frequency to 0.2 mm/μs. In our case, a volume fraction of 0.4% suggested V = 0.4%**x**150ml = 0.6 ml; by assuming that all bubbles have a diameter of 1mm, $V = 4/3N\pi <0.5\ mm>^3 = 0.6$ ml and N ~1150 bubbles: 10^3 bubbles inside an SED would be sufficient to cause attenuation of the sound amplitude.

A new set of experiments with the larger DSD was performed to examine the event rate decrease with time, in which a recompressed detector with 3Bq U was left to count for 6 - 24 h at fixed temperatures of 10 °C, 11 °C and 12 °C; after each temperature run, the SED was recompressed at 20 bar for 4 h.

As seen in Fig. 11, the initial rate increases with temperature increase: 10 °C (868 bubbles); 11 °C (1559 bubbles); 12 °C (2192 bubbles). A fresh/recompressed SED records less than the model prediction for the first minute of acquisition (38.13 evt/g/min instead of 84 evt/g/min predicted by the

model at 10 °C; 93.53 #/g/min instead of 132.27 #/g/min and 109.15 #/g/min instead of 156.50 #/g/min at 12 °C). This could be due to some active mass loss during long previous acquisitions but this effect could only explain few % changes in the counting rate. As seen in Fig. 12(a), the initial rate (R_0) increases with temperature increase.

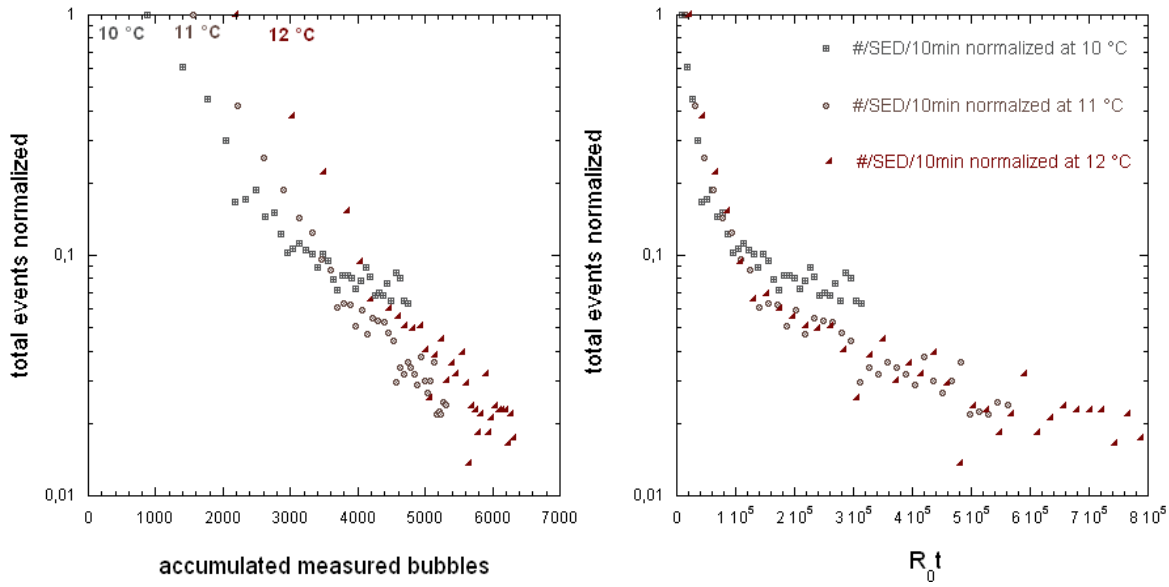

(a) (b)

Fig. 11: (a) event rate normalized to 1 as a function of the number of bubbles accumulated inside the SED at 3 different temperatures for 6 h acquisition each: square = 10 °C, circles = 11 °C; triangle = 12 °C; (b) total events normalized to 1 versus the initial nucleation rate R_0t at the three different temperatures for 6 h acquisition each. The three curves superimpose, indicating an universal behavior.

By replacing the number of recorded bubbles by R_0t, which represents the constant event rate without attenuation, all curves superimpose as seen in Fig. 11(b). The decreasing event rate does not depend on acquisition time or accumulated bubbles, but on both R_0t, i.e. the hypothetical number of bubbles inside the SED assuming that the nucleation rate is R_0. The signal attenuation becomes evident after 10^3 bubbles.

4.3 Final Results

With the addition of attenuation, Eq. (4) becomes:

$$\tau_\alpha(p_< \leftrightarrow T) = \frac{1}{2}\varepsilon_{at} A_0 \sum_{k_\alpha} f_{k_\alpha} \varepsilon(p_<) F(p_<) \quad . \tag{7}$$

with the additional attenuation efficiency ε_{at} determined from the measurements of Sec. 4.2.

These are shown in Fig. 12, in comparison with the experiments, for the two uranium concentrations. In Fig. 12(a) only the model results for the larger DSD (dotted line) are displayed. There is good agreement between the attenuated event rate and the experiments at 3 Bq until 10 ºC.

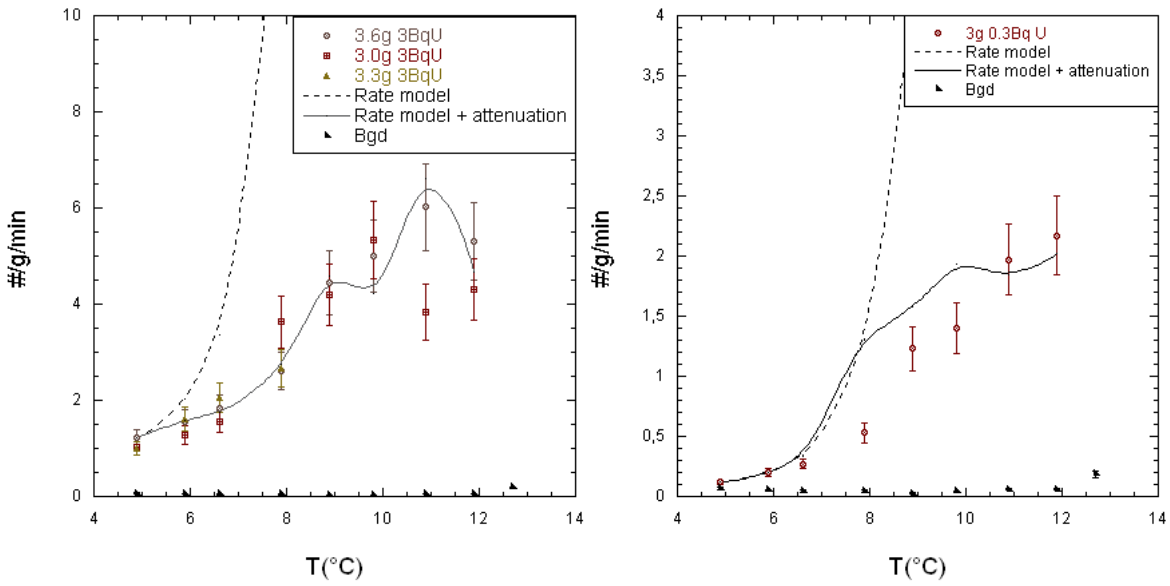

(a) (b)

Fig. 12: (a) 3 Bq U and (b) 0.3 BqU; the theoretical event rate (dotted) and model (grey) of Eq. (7).

No long run experiments were made in the case of the 0.3 Bq SED; the universal behavior of Fig. 11(b) is assumed.

The spectral nature of Fig. 12 (a) and 12(b) is shown in Fig. 13(a), which displays the temperature differential of the responses and fitted contours for the two peaks. The spectrum of Fig. 13(a) indicates the two peaks of the uranium irradiation of the smaller DSD (SED 3.6 g; 3 Bq U and SED 3.0 g; 0.3 Bq U) to overlap, with the ^{234}U α occurring ~ 2 °C after the ^{238}U α, as predicted by Figure 13(b). The peaks of the larger DSD (SED 3.0 g; 3 Bq U) show a downward shift of 1 °C compared to the smaller, as expected from Fig. 13(b) with a DSD centered at 10 µm diameter.

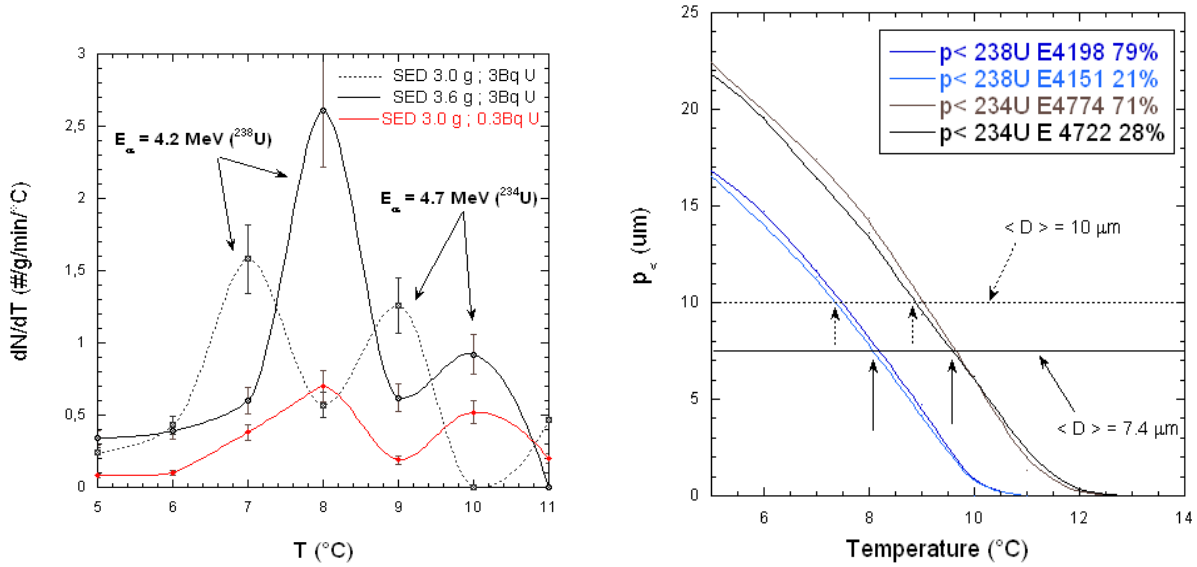

(a) (b)

Fig. 13: (a) α-irradiation response spectra of Fig. 9: the smaller DSDs are seen to yield spectra shifted by ~1 ºC above that of the larger DSD; (b) the minimum depth penetration vs. temperature with two DSDs centered at 10 µm and 7.4 µm diameter: the arrows show the predicted detection temperature of each α energy for each DSD.

5. CONCLUSIONS

We have studied the response of C_2ClF_5-based SEDs to α's of natural uranium and samarium decays both experimentally and using a geometric model based on droplet surface emission. The results confirm that the detector DSD has an impact on α detection, and that by increasing the droplet sizes to a higher mean radius the α detection is shifted to lower temperature. The addition of a sound attenuation correction to the model resulting from the increasing bubble population is seen to increase the agreement between model and experiment.

The model is simple: it is restricted to only surface α-emission, neglecting contribution from non-actinide emitters. It also does not account for α-emission near the droplet surface, which although estimated to contribute at < 1.5% would decrease the $p_<$ to alter the response. The Bragg curves, from which the $p_<$ are determined, are track-averages over calculated particle trajectories, and do not allow for statistical variations of the SED response. The disagreement with the attenuation-corrected rate at temperatures above 10 ºC suggests the contribution of effects beyond signal attenuation not considered here, to possibly include Ostwald ripening, bubble deformation, fractures, and temperature effects on the DSD and gel. Although further investigation of all is required, the model is nevertheless seen to

provide a basic description of the SED response which reproduces to a large extent the experimental results, and offers guidance in SED construction and utilization.

Figure 13(a) provides the basis for an α-spectroscopy with SEDs. The temperature shift of the same-energy α's in the Figure is because of the difference in DSD. By tuning the DSD to a well known value, the energies of the α's can be retrieved. The number of spikes determines the composition of the isotopes of the sample. Reduction in the DSD width and/or smaller temperature steps (or slow ramping) would improve the resolution

The effect of the droplet size on the α-response suggests an α-spectrometer construction with a well known DSD. Larger DSD would be sensitive to higher α energy**,** but depending on $p_>$ also to other lower energy α's. The dependence of $p_<$ on temperature correlates the "kinks" in the SED response function with E_α. For example, in Fig. 12 & 13, the two-fold increase in the signal at 8 ^oC corresponds to the emergence of the ^{234}U contribution. By tuning the DSD to a diameter of 15 µm, for example, only 4.15 MeV α's would trigger the droplet at 5 °C; by increasing the droplet size to 20 µm at the same temperature, the detection would be for both 4.72 MeV and 4.15 MeV α's since the $p_>$(5 °C) = 26 µm is the maximum penetration length of an α to trigger the droplet. This means that by increasing the droplet size, the detection of higher E_α (the case for natural thorium contamination) is increased. In the case of C_2ClF_5, only α from a few to 5 MeV will be detectable. For higher E_α, a larger droplet would be necessary -- but smaller E_α would also trigger nucleation depending on the $p_>$.

Acknowledgements

We thank Dr. Luis Cerqueira Alves for use of his optical microscope, and Dr José Vieira Antunes for helpful discussion regarding the acoustic attenuation. This work was funded by projectsIF/00628/2012/CP0171/CT0008and PTDC/EEI-ELC/2468/2014 of the Portuguese Foundation for Science and Technology (FCT). The activit~~i~~es of Morlat and Felizardo are supported by FCT project UID/Multi/04349/2013 and grant SFRH/BPD/94028/2013, respectively.

References:

[1] F. d'Errico, Radiation Dosimetry and Spectrometry with Superheated Emulsions, Nucl. Instrum. Meth. B184 (2001) 229.

[2] M.J. Harper and J.C. Rich, Radiation-induced Nucleation in Superheated Liquid Droplet Neutron Detectors, Nucl. Instrum. Methods A336 (1993) 220.

[3] H. Ing, R.A. Noulty, T.D. McLean, Bubble Detectors - A Maturing Technology, Radiation Measurements 27 (1997) 1-11

[4] H.W. Bonin, G.R. Desnoyers, T. Cousins, Fast Neutron Dosimetry and Spectroscopy Using Bubble Detectors, Radiat. Prot. Dosim. 46 (2001) 265.

[5] M. Das and T. Sawamura, Superheated Emulsions in Neutron Spectrometry by Varying Ambient Pressure, Nucl. Instrum. Meth. A536 (2005) 123.

[6] M. Felizardo *et al*., Phase II of the SIMPLE Dark Matter Search, Phys. Rev. D89 (2014) 072013.

[7] E. Behnke et al., Final Results of the PICASSO Dark Matter Search Experiment, Astroparticle Physics 90 (2017) 85.

[8] M. Felizardo *et al*, Nuclear Recoil-α Event Discrimination in Superheated Emulsion Detectors, Nucl. Instrum. Meth. A863 (2017) 62-73.

[9] S. Archambault, F. Aubin, M. Auger, et al., New Insights into Particle Detection with Superheated Liquids, New J. Phys. 13 (2011) 043006.

[10] L. K. Pan, C.-K.C. Wang, Superheated-Liquid-Droplet Technique for Measuring Alpha Decays in Uranium Solutions, Nucl. Instrum. Meth. A420 (1999) 345.

[11] S. Seth and M. Das, Radiation LET and Drop Size Dependence of the Low Frequency Signal from Tiny Superheated Droplets, Nucl. Instrum. Meth. A837 (2016) 92.

[12] S. Seth and M. Das, The Simulation of the Response of Superheated Emulsion to Alpha Particles,JINST 11 (2016) no.04, P04015.

[13] Table of Isotopes: ed. R.B. Firestone, V.S. Shirley, C.M. Baglin; S.Y.F. Chu, J. Zipkin (John Wiley & Sons, Inc.), 1976

[14] F. Seitz, On the Theory of the Bubble Chamber, Phys. Fluids 1 (1958) 2.

[15] J. Ziegler, Stopping and Range of Ions in Matter: http://www.srim.org/

[16] J.E. Grindler, The Radiochemistry of Uranium (National Academy of Science-National Research Council, Washington, 1962).

[17] A.L. Mills, D.H. Logsdail, Solvent Extraction and Ion Exchange in the Nuclear Fuel Cycle, (Ellis Horwood Limited, London, 1985).

[18] P.A.G. OÕhare, E.H.P. Cordfunke, The Chemical Thermodynamics of Actinide Elements and Compounds, Part3 Miscellaneous Actinide Compounds (International Atomic Energy Agency, Vienna, 1978).

[19] - M. Felizardo et al., "New Acoustic Instrumentation for the SIMPLE Superheated Droplet Detector", Nuclear Instruments and Methods in Physics Research A 589 (2008) 72-84, doi: 10.1016/j.nima.2008.02.012.

[20] V. Leroy et al., Sound Velocity and Attenuation in Bubbly gels Measured by Transmission Experiments, J. Acoust. Soc. Am. **123** (4), April 2008.

[21] M. Kafesaki *et al*, Air Bubbles in Water: A Strongly Multiple Scattering Medium for Acoustic Waves, Phys. Rev. Lett. Vol. 84, Nb 26, 26 June 2000.

[22] Zhen Ye and Alberto Alvarez, Acoustic Localization in Bubbly Liquid Media, Phys. Rev. Lett. Vol. 80, Number 16, 20 April 1998.

[23] J. Puibasset, Étude de Suspensions de Gouttelettes de Fréon en Surchauffe en Vue de la Réalisation d'un Détecteur de Matiére Cachée Galactique, PhD thesis, Univ. Paris VII, 2000 (unpublished).